Wind and Structures, Vol. 10, No. 5 (2007) 463-479
DOI: http://dx.doi.org/10.12989/was.2007.10.5.463

Wind-induced self-excited vibrations of a twin-deck bridge and the effects of gap-width

X.R. Qin†

CLP Power Wind/Wave Tunnel Facility, The Hong Kong University of Science and Technology, Clear Water Bay, Kowloon, Hong Kong, China
Institute of Mechanical Design and Its Theory, School of Mechanical Engineering, Tongji University, 1239 Si-Ping Road, Shanghai, 200092, China

K.C.S. Kwok, C.H. Fok and P.A. Hitchcock

CLP Power Wind/Wave Tunnel Facility, The Hong Kong University of Science and Technology, Clear Water Bay, Kowloon, Hong Kong, China

Y.L. Xu

Department of Civil and Structural Engineering, The Hong Kong Polytechnic University, Hung Hom, Kowloon, Hong Kong, China

(Received March 29, 2006, Accepted October 24, 2006)

Abstract. A series of wind tunnel sectional model dynamic tests of a twin-deck bridge were conducted at the CLP Power Wind/Wave Tunnel Facility (WWTF) of The Hong Kong University of Science and Technology (HKUST) to investigate the effects of gap-width on the self-excited vibrations and the dynamic and aerodynamic characteristics of the bridge. Five 2.9 m long models with different gap-widths were fabricated and suspended in the wind tunnel to simulate a two-degrees-of-freedom (2DOF) bridge dynamic system, free to vibrate in both vertical and torsional directions. The mass, vertical frequency, and the torsional-to-vertical frequency ratio of the 2DOF systems were fixed to emphasize the effects of gap-width. A free-vibration test methodology was employed and the Eigensystem Realization Algorithm (ERA) was utilized to extract the eight flutter derivatives and the modal parameters from the coupled free-decay responses. The results of the zero gap-width configuration were in reasonable agreement with the theoretical values for an ideal thin flat plate in smooth flow and the published results of models with similar cross-sections, thus validating the experimental and analytical techniques utilized in this study. The methodology was further verified by the comparison between the measured and predicted free-decay responses. A comparison of results for different gap-widths revealed that variations of the gap-width mainly affect the torsional damping property, and that the configurations with greater gap-widths show a higher torsional damping ratio and hence stronger aerodynamic stability of the bridge.

Keywords: wind-induced vibration; flutter derivative; system identification; twin-deck bridge; wind tunnel dynamic test.

† Corresponding Author, E-mail: xianrongqin@hotmail.com

1. Introduction

Long-span flexible bridges are quite sensitive to wind loads. Therefore, their potential wind-induced vibrations must be carefully predicted before construction. Due to the complex characteristics of the wind and the bridge structures, it is not surprising that bridges will experience a variety of wind-induced vibrations in the natural wind field. However, it is first necessary to ensure that the bridge is aerodynamically stable and to avoid the potentially destructive vibrations, such as flutter.

According to Sato, *et al*. (1995 and 2000) and Matsumoto, *et al*. (2004), a slotted bridge deck has good flutter characteristics and provides a possible method of improving flutter stability and thus increasing the flutter speed of a bridge. Efforts were also made by the aforementioned researchers to explain the reason for the good performance of slotted bridges. Sato, *et al*. (2000) employed wind tunnel dynamic tests to investigate the behaviour of the slotted bridges in the coupled physical space by estimating the unsteady aerodynamic forces of such structures. Xiang and Ge (2002) also investigated the behaviour using a Computational Fluid Dynamics (CFD) approach. Matsumoto, *et al*. (2004), however, turned to the static wind tunnel pressure tests to study the pressure distribution on the surface of slotted bridges. In this paper, the behaviour was viewed from a different point, and the characteristics of slotted bridges were investigated in both the uncoupled modal space and the coupled physical space, to gain further understanding of the problems, i.e., why do slotted decks possess better flutter characteristics?

In this paper, the effects of gap-width on the modal parameters (in the uncoupled modal space), and subsequently the flutter derivatives (in the coupled physical space) of a real twin-deck cable-stayed bridge, were investigated in a series of wind tunnel dynamic tests. Five 2.9 m long sectional models of the bridge were fabricated with different gap-widths, but with identical cross-sectional shape and chord length. The test models were supported by a custom designed rig-spring mechanism. The models were excited by applying an initial displacement and allowed to vibrate in the vertical and torsional directions.

A popular time-domain deterministic identification method, the Eigensystem Realization Algorithm (ERA, Juang and Pappa 1985), an identification algorithm with clear physical meanings and good noise-resistance capability, was employed to extract the dynamic and aerodynamic parameters from the coupled free-decay responses of the models. The results of the zero gap-width configuration were compared with the theoretical values for an ideal thin flat plate in smooth flow and other published results for models with similar cross-sectional shape to validate the experimental and analysis methodologies. The measured free-decay responses for Gap 1 were compared with the responses predicted by the identified parameters to further validate the effectiveness of the methodologies. The results of all the five gap-width configurations were also compared to determine the effects of gap-width on the dynamic modal parameters and the aerodynamic stability of the model.

2. Basic formulations

At a specific wind speed, the motion of a bridge deck with two-degrees-of-freedom (2DOF), i.e., vertical bending (h) and torsion (α), in smooth flow can be modelled as:

$$[M]\{\ddot{y}(t)\} + [C^0]\{\dot{y}(t)\} + [K^0]\{y(t)\} = \{F_{se}(t)\} \tag{1}$$

in which: $[M]$, $[C^0]$, and $[K^0]$ are the structural mass, damping and stiffness matrices of the 2DOF bridge dynamic system per unit span; $\{y\}=[h, \alpha]^T$ is the displacement response vector; and $\{F_{se}]=[L_{se}, M_{se}]^T$ is the self-excited force vector, where L_{se} and M_{se} are the self-excited lift force (N/m) and pitching moment (N·m/m) respectively per unit span of bridge, as given by Scanlan (1971) and Sarkar, *et al*. (1994):

$$\begin{aligned} L_{se}(t) &= \rho U^2 B\left[KH_1^*(K)\frac{\dot{h}(t)}{U} + KH_2^*(K)\frac{B\dot{\alpha}(t)}{U} + K^2H_3^*(K)\alpha(t) + K^2H_4^*(K)\frac{h(t)}{B}\right] \\ M_{se}(t) &= \rho U^2 B^2\left[KA_1^*(K)\frac{\dot{h}(t)}{U} + KA_2^*(K)\frac{B\dot{\alpha}(t)}{U} + K^2A_3^*(K)\alpha(t) + K^2A_4^*(K)\frac{h(t)}{B}\right] \end{aligned} \tag{2}$$

in which ρ is air density (kg/m^3); U is the approach mean wind speed (m/s); B is the bridge deck width (m); K is the dimensionless reduced frequency, and is defined as $K=\omega B/U$; where ω is the circular vibration frequency (rad/s) at wind speed U; H_i^* and A_i^*, $(i=1, 2, 3, 4)$, are the dimensionless flutter derivatives.

By moving the self-excited force to left-hand side and incorporating the "coefficients" of each variable, Eq. (1) can be rewritten as Eq. (3), in which $\{n\}$ is a null column vector, i.e., $\{n\}=[0, 0]^T$; $[C^e]$ and $[K^e]$ are the damping and stiffness matrices aerodynamically modified by the self-excited lift force and pitching moment. It is noteworthy that $[C^e]$ and $[K^e]$ are asymmetrical.

$$[M]\{\ddot{y}(t)\} + [C^e]\{\dot{y}(t)\} + [K^e]\{y(t)\} = \{n\} \tag{3}$$

For a 2DOF bridge dynamic system modelled by Eq. (3), it is possible to decompose both its free vibration displacements and the self-excited forces into two parts, associated with the vertical and torsional complex modes, respectively:

$$\begin{aligned} \{y(t)\} &= \{y_h(t)\} + \{y_\alpha(t)\} \\ \{F_{se}(t)\} &= \{F_{seh}(t)\} + \{F_{se\alpha}(t)\} \end{aligned} \tag{4}$$

Eq. (3) therefore can be decomposed into the following two matrix equations (Chen and Kareem 2004):

$$[M]\{\ddot{y}_h(t)\} + [C^e(K_h)]\{\dot{y}_h(t)\} + [K^e(K_h)]\{y_h(t)\} = \{n\} \tag{5}$$

$$[M]\{\ddot{y}_\alpha(t)\} + [C^e(K_\alpha)]\{\dot{y}_\alpha(t)\} + [K^e(K_\alpha)]\{y_\alpha(t)\} = \{n\} \tag{6}$$

in which $\{y_h(t)\}$, $[C^e(K_h)]$ and $[K^e(K_h)$ are the displacement vector, damping matrix and stiffness matrix associated with the vertical complex mode, and $\{y_\alpha(t)$, $[C^e(K_\alpha)]$ and $[K^e(K_\alpha)]$ are those associated with the torsional complex mode. It can be concluded from Eq. (2) to Eq. (6) that the free vibrations of the 2DOF bridge dynamic system correspond to two sets of eight flutter derivatives (sixteen in total) associated with the vertical and torsional complex modes respectively. Since, from the point of structural dynamics, the free vibrations of a 2DOF dynamic system cannot provide sufficient information to uniquely determine sixteen independent variables, approximations have to be made to solve the problem (Sarkar, *et al*. 1994, Iwamoto and Fujino 1995, Gu, *et al*. 2000):

$$[C^e(K_h)] \approx [C^e(K_\alpha)] \approx [C^{ef}] = \begin{bmatrix} C^e_{hh}(K_h) & C^e_{h\alpha}(K_\alpha) \\ C^e_{\alpha h}(K_h) & C^e_{\alpha\alpha}(K_\alpha) \end{bmatrix} \tag{7}$$

$$[K^e(K_h)] \approx [K^e(K_\alpha)] \approx [K^{ef}] = \begin{bmatrix} K^e_{hh}(K_h) & K^e_{h\alpha}(K_\alpha) \\ K^e_{\alpha h}(K_h) & K^e_{\alpha\alpha}(K_\alpha) \end{bmatrix} \tag{8}$$

Therefore, the governing equations of motion of the 2DOF bridge dynamic system can be approximated by Eq. (9), which is deduced by substituting the effective damping matrix $[C^{ef}]$ and the effective stiffness matrix $[K^{ef}]$ for $[C^e(K_h)]$ and $[K^e(K_h)]$ in Eq. (5) and for $[C^e(K_\alpha)]$ and $[K^e(K_\alpha)]$ in Eq. (6), and summing the results to arrive at:

$$[M]\{\ddot{y}(t)\} + [C^{ef}]\{\dot{y}(t)\} + [K^{ef}]\{y(t)\} = \{n\} \tag{9}$$

Eq. (9) and the approximations made in Eq. (7) and Eq. (8) actually imply that at a specific wind speed, the self-excited lift force and pitching moment of the 2DOF bridge dynamic system can be approximated by Eq. (10), leaving only eight independent flutter derivatives.

$$\begin{aligned} L_{se}(t) &= \rho U^2 B\left[K_h H_1^*(K_h)\frac{\dot{h}(t)}{U} + K_\alpha H_2^*(K_\alpha)\frac{B\dot{\alpha}(t)}{U} + K_\alpha^2 H_3^*(K_\alpha)\alpha(t) + K_h^2 H_4^*(K_h)\frac{h(t)}{B}\right] \\ M_{se}(t) &= \rho U^2 B^2\left[K_h A_1^*(K_h)\frac{\dot{h}(t)}{U} + K_\alpha A_2^*(K_\alpha)\frac{B\dot{\alpha}(t)}{U} + K_\alpha^2 A_3^*(K_\alpha)\alpha(t) + K_h^2 A_4^*(K_h)\frac{h(t)}{B}\right] \end{aligned} \tag{10}$$

It is also possible for Eq. (9) to be expressed by the following state equations:

$$\begin{aligned} \{\dot{x}(t)\} &= [A]\{x(t)\} \\ \{y(t)\} &= [C]\{x(t)\} \end{aligned} \tag{11}$$

in which $\{x\} = [y, \dot{y}]^T$ is the state vector; $[A]$ and $[C]$ are the state and output matrices, respectively. In discrete-time space, Eq. (11) would be converted into the following form:

$$\begin{aligned} \{x(k+1)\} &= [A_D]\{x(k)\} \\ \{y(k)\} &= [C]\{x(k)\} \end{aligned} \tag{12}$$

where $\{x(k=1)\}$ and $\{x(k)\}$ are the states at time instant $(k+1)\Delta t$ and $k\Delta t$; $\{y(k)\}$ is the response at time $k\Delta t$, where Δt is the sampling time interval (s). $[A_D]$ is the state matrix in discrete-time space. Therefore, the response of the bridge to an initial state $\{x(0)\}$, the free-decay response, can be written as:

$$\{y(k)\} = [C][A_D]^k\{x(0)\} \qquad (k>0) \tag{13}$$

By forming the block Hankel matrix,

$$H_{rs}(k-1)] = \begin{bmatrix} \{y(k)\} & \{y(k+1)\} & \dots & \{y(k+s)\} \\ \{y(k+1)\} & \{y(k+2)\} & \dots & \{y(k+s+1)\} \\ \vdots & \vdots & & \vdots \\ \{y(k+r)\} & \{y(k+r+1)\} & \dots & \{y(k+s+r)\} \end{bmatrix} \tag{14}$$

the state matrix $[A_D]$ can be determined by the Eigensystem Realization Algorithm (ERA) presented by Juang and Pappa (1985):

$$[A_D] = [S]^{-1/2}[P]^T[H_{rs}(1)][Q][S]^{-1/2} \tag{15}$$

in which the subscripts r and s are the number of row and column shifts of the Hankel matrix, respectively, and $[P]$, $[S]$ and $[Q]$ are matrices used to construct the pseudo-inverse of $[H_{rs}(0)]$ and are determined by the following singular value decomposition (SVD):

$$[H_{rs}(0)] = [P][S][Q]^T \tag{16}$$

By solving the eigenvalue problem of the state matrix $[A_D]$ and converting the eigen-pairs into continuous-time space, the modal parameters of the bridge deck can be determined. Subsequently, the state matrix $[A]$ in Eq. (11), and then the effective damping and stiffness matrices $[C^{ef}]$ and $[K^{ef}]$, can be estimated by the pseudo-inverse technique. The flutter derivatives can then be obtained by comparing $[C^{ef}]$ and $[K^{ef}]$ with $[C^0]$ and $[K^0]$, the damping and stiffness matrices at zero wind speed:

$$\begin{aligned} H_1^*(K_h) &= -\frac{m}{\rho B^2 \omega_h}(\tilde{C}_{hh}^{ef} - \tilde{C}_{hh}^0) & A_1^*(K_h) &= -\frac{I}{\rho B^3 \omega_h}(\tilde{C}_{\alpha h}^{ef} - \tilde{C}_{\alpha h}^0) \\ H_2^*(K_\alpha) &= -\frac{m}{\rho B^3 \omega_\alpha}(\tilde{C}_{h\alpha}^{ef} - \tilde{C}_{h\alpha}^0) & A_2^*(K_\alpha) &= -\frac{I}{\rho B^4 \omega_\alpha}(\tilde{C}_{\alpha\alpha}^{ef} - \tilde{C}_{\alpha\alpha}^0) \\ H_3^*(K_\alpha) &= -\frac{m}{\rho B^3 \omega_\alpha^2}(\tilde{K}_{h\alpha}^{ef} - \tilde{K}_{h\alpha}^0) & A_3^*(K_\alpha) &= -\frac{I}{\rho B^4 \omega_\alpha^2}(\tilde{K}_{\alpha\alpha}^{ef} - \tilde{K}_{\alpha\alpha}^0) \\ H_4^*(K_h) &= -\frac{m}{\rho B^2 \omega_h^2}(\tilde{K}_{hh}^{ef} - \tilde{K}_{hh}^0) & A_4^*(K_h) &= -\frac{I}{\rho B^3 \omega_h^2}(\tilde{K}_{\alpha h}^{ef} - \tilde{K}_{\alpha h}^0) \end{aligned} \tag{17}$$

in which:

$$\begin{aligned} [\tilde{C}^e] &= [M]^{-1}[C^e] & [\tilde{K}^e] &= [M]^{-1}[K]^e \\ [\tilde{C}^0] &= [M]^{-1}[C^0] & [\tilde{K}^0] &= [M]^{-1}[K]^0 \end{aligned} \tag{18}$$

and m and I are the mass (kg/m) and mass moment of inertia ($\mathrm{kg \cdot m^2/m}$) of the 2DOF bridge dynamic system per unit span of the bridge.

Therefore, the eight flutter derivatives, as defined in Eq. (10), at a specific wind speed can be determined by:

(i). Extracting the natural modal parameters from the free-decay responses at zero wind speed by ERA and determining the structural stiffness and damping matrices by the resultant modal parameters;
(ii). Extracting the modal parameters from the free-decay responses at the specific wind speed by ERA and determining the effective stiffness and damping matrices $[K^{ef}]$ and $[C^{ef}]$ by the resultant modal parameters;
(iii). Determining flutter derivatives by Eq. (17).

3. Wind tunnel dynamic tests

3.1. Model, tests and data acquisition procedures

To investigate the effects of gap-width on the dynamic and aerodynamic characteristics of a real twin-deck cable-stayed bridge, five 2.9 m long, nominally rigid sectional models of the bridge were fabricated to produce gap-width (b) to total width (B) ratios of 0% (Gap 1, i.e. zero gap), 2.4% (Gap 2), 16% (Gap 3), 27% (Gap 4) and 35% (Gap 5), with the individual chord dimensions of the bridge properly simulated. Fig. 1 shows the cross-sectional shape of the models, and Table 1 lists the corresponding dimensions of different configurations at model scale.

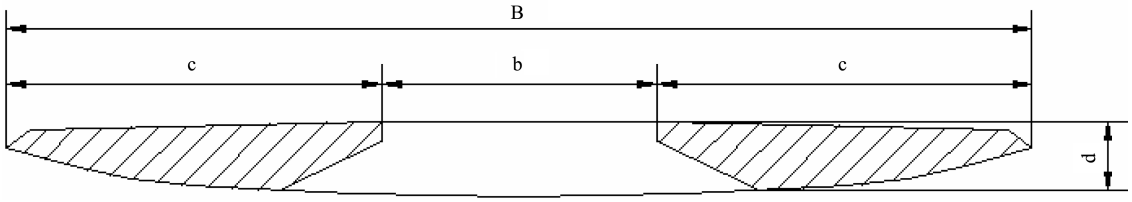

Fig. 1 Cross-sectional shape of the tested sectional bridge model

Table 1 Dimensions of the bridge sectional models at model scale (unit: mm)

	Gap 1	Gap 2	Gap 3	Gap 4	Gap 5
Deck width (B)	488	500	581	666	751
Deck depth (d)	44	44	44	44	44
Chord width (c)	244	244	244	244	244
Gap-width (b)	0	12	93	178	263

The test models were elastically suspended by a custom-designed rig-spring mechanism, as shown in Fig. 2, in the high-speed test section of a boundary layer wind tunnel with a cross-section of 3 m (width) by 2 m (height) at the CLP Power Wind/Wave Tunnel Facility (WWTF) at The Hong Kong University of Science and Technology (HKUST) to simulate a 2DOF bridge dynamic system that is free to vibrate in the vertical bending and torsion directions. The mass, mass moment of inertia about center of mass, vertical natural frequency and torsional-to-vertical frequency ratio of the 2DOF bridge dynamic system were kept nearly constant to emphasize the effects of gap-width. The ratio of the torsional-to-vertical natural frequency of the bridge dynamic system was about 2.2:1, where the vertical natural frequency was approximately 1.72 Hz.

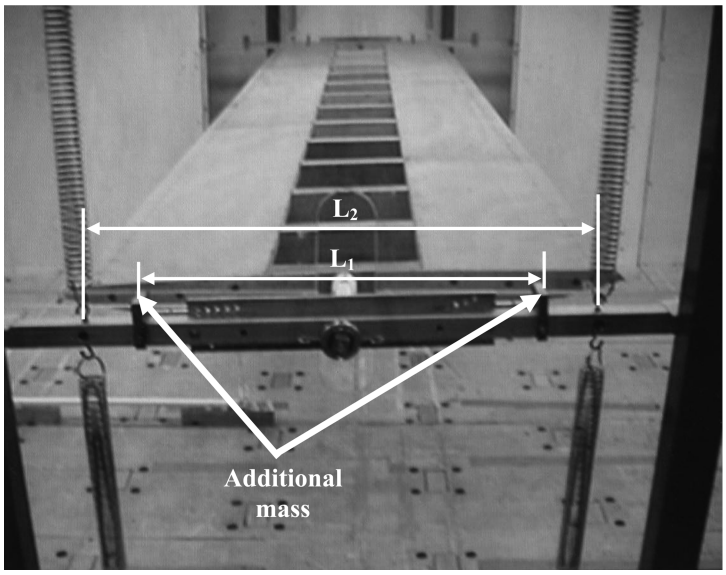

Fig. 2 Bridge sectional model suspended by a custom-designed rig-spring mechanism

The mass of the 2DOF bridge dynamic system comprised the mass of the bridge sectional model, the mass of the custom-designed rig-spring mechanism, and additional mass, as shown in Fig. 2. The total stiffness of all the springs was determined by the required mass, the mass of the twin-deck bridge at model scale, and the vertical natural frequency of the 2DOF bridge dynamic system. Subsequently, the required torsional-to-vertical natural frequency ratio was obtained by fine-tuning the space between the additional mass (L_1 in Fig. 2) and the space between the springs (L_2 in Fig. 2). The mass moment of inertia of the bridge dynamic system was simply calculated from the torsional natural frequency, the stiffness of the springs, and the space between the springs.

The models were tested at zero angle of wind incidence and at zero inclination only, in smooth flow, with a turbulence intensity less than 1%, and at wind speeds ranging from 1 m/s up to the approximate design mean wind speed of the prototype bridge (10 m/s at model scale) at 1 m/s intervals. Four laser sensors, denoted as s_1, s_2, s_3 and s_4 in Fig. 3, were set up at both ends of the bridge model to record its displacement responses, which were subsequently used to extract the

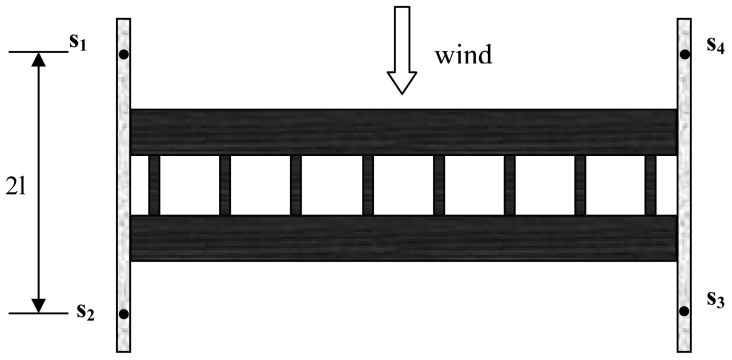

Fig. 3 Top view of the positions of laser sensors (s_1, s_2, s_3 and s_4) to measure the vertical displacement responses

corresponding vertical (h) and torsional (α) free-decay responses of the model:

$$h = \frac{z_1 + z_3}{2} \qquad \alpha = \frac{z_2 - z_1}{2l} \tag{19}$$

in which z_1, z_2 and z_3 are the displacement responses (m) of the bridge model recorded by sensor s_1, s_2 and s_3, respectively, and $2l$ is the distance between sensor s_1 and sensor s_2, the two sensors at the same end of the model.

To excite the model, a strong string was attached to the bridge model to give it an initial displacement. The coupled free-decay responses of the model were sampled at a rate of 100 Hz for a period of 70 seconds and were low-pass filtered at 50 Hz. ERA was subsequently employed to extract the modal parameters and the eight flutter derivatives of the model from its coupled free-decay responses. The sampling and identifying processes were each repeated five times to minimize the potential effects of noise and to give the average values of the corresponding parameters.

3.2. Methodology verification

The Eigensystem Realization Algorithm (ERA), which was utilized by Qin and Gu (2004) and

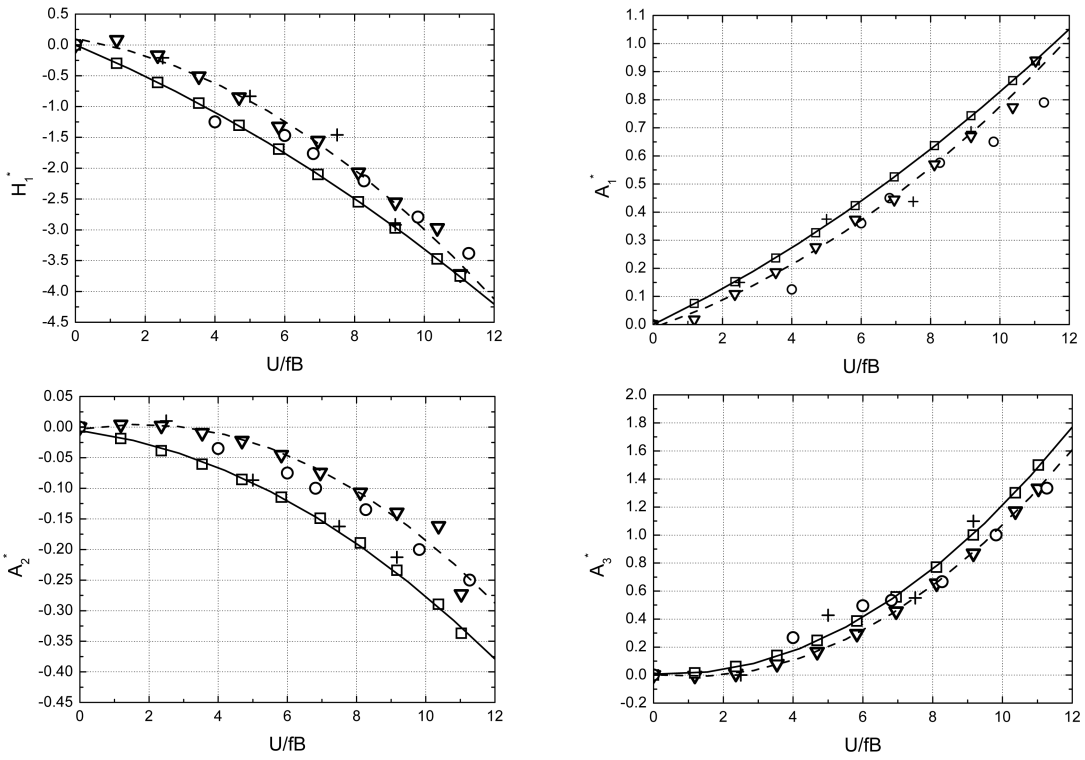

Fig. 4 Flutter derivatives of zero gap-width configuration in comparison with previously published results
—— : thin flat plate (Scanlan) ------ : Gap 1 (curve fitted) ∇: Gap 1
□ : thin flat plate (Scanlan 1971) + : thin flat plate (Gu, *et al*. 2000)
○ : streamline bridge deck (Sarkar, *et al*. 1994)

proven to be an effective means of determining the natural properties of a 2DOF bridge model, was employed in the current study to determine the natural properties and the aerodynamic parameters of the 2DOF bridge dynamic system tested. Before any application to further investigations, the wind tunnel test techniques and data analysis programs were verified and benchmarked.

According to Scanlan's theory (1971), flutter derivatives of an ideal thin flat plate in smooth flow can be defined by Theodorson's functions. As shown in Fig. 1 and Table 1, the cross-sectional shape of the tested sectional model with zero gap-width (Gap 1) had a width (B) to depth (d) ratio

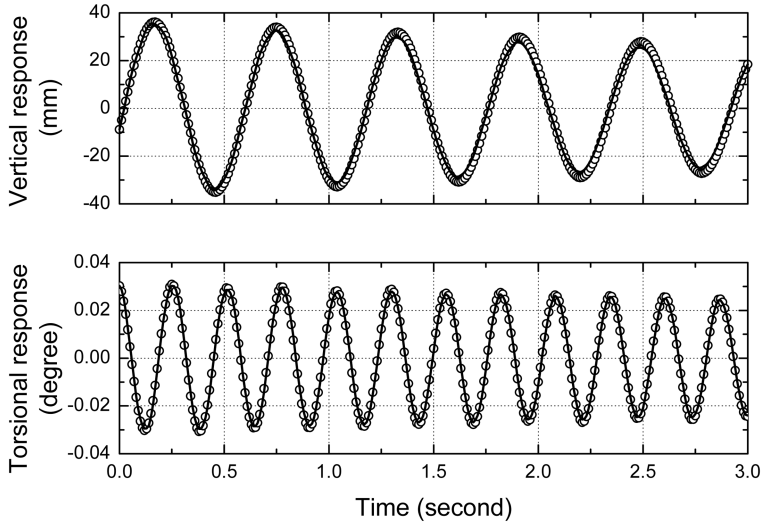

(a). 0 m/s wind speed

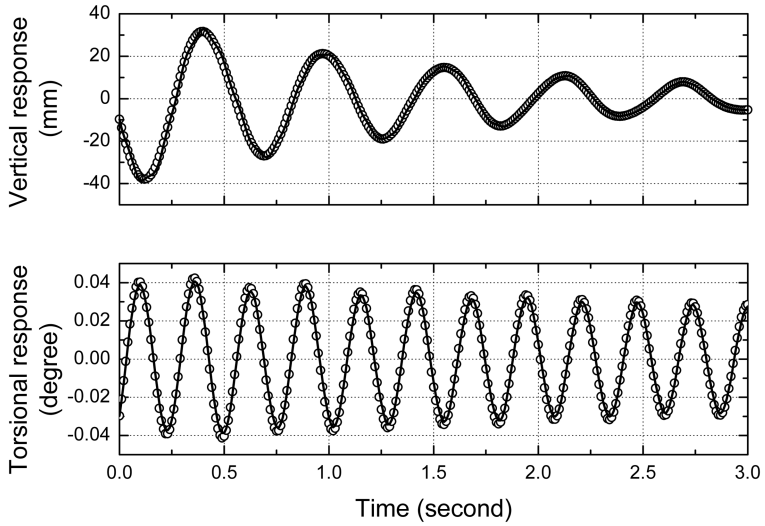

(b). 5 m/s

Fig. 5 Segments of measured free-decay responses for Gap 1 in comparison with those predicted by the identified stiffness and damping matrices
——: measured responses ○ : predicted responses

of about 11:1, and is of similar geometrical proportions to a thin flat plate and should thus have similar aerodynamic properties. Fig. 4 shows the identified four important flutter derivatives H_1^*, A_1^*, A_2^* and A_3^* of the tested zero gap-width configuration compared with the corresponding theoretical values (Scanlan, 1971) and the published results of models with similar cross-sectional shapes (Sarkar 1994 and Gu 2000). All the results in Fig. 4 were normalized by the actual vertical vibration frequencies of the models at specific test wind speeds. The reasonable agreement between the current study and the previously published results highlights the effectiveness of the experimental and data analysis techniques utilized.

The analytical procedures used in this study were also verified further by comparing measured and predicted free-decay responses of the Gap 1 configuration at different wind speeds. The responses of a given time-invariant dynamic system, modelled by its state matrix $[A_D]$ and the input matrix $[C]$, to an initial state $\{x(t_0)\}$ can be readily calculated according to Eq. (12). For the current study, the stiffness and damping matrices of the 2DOF bridge dynamic system at a specific wind speed can be extracted from the measured free-decay responses by the methodology described in Section 2, and the initial state can be determined from the responses of the system measured at a time instant t_0. The responses of the system after t_0 therefore can be predicted according to Eq. (12).

Fig. 5 presents the comparison of the measured and predicted free-decay responses for Gap 1, at 0 m/s and 5 m/s. To highlight the differences between the measured and predicted responses, only a short segment of the responses was shown in Fig. 5. The predicted responses matched very closely with the responses measured at each corresponding time instant, which further verifies the effectiveness of the experimental and data analysis techniques employed.

3.3. Identified modal frequencies and damping ratios

Fig. 6 and Fig. 7 present the identified modal frequencies and modal damping ratios, respectively, of the vertical and torsional complex modes of models with different gap-widths. Although the modal frequencies of the vertical and torsional modes showed slight increases and decreases with wind speed, respectively, in comparison with the damping ratios, overall the modal frequencies were relatively insensitive to the variations of gap-width. In contrast, the modal damping ratio of the

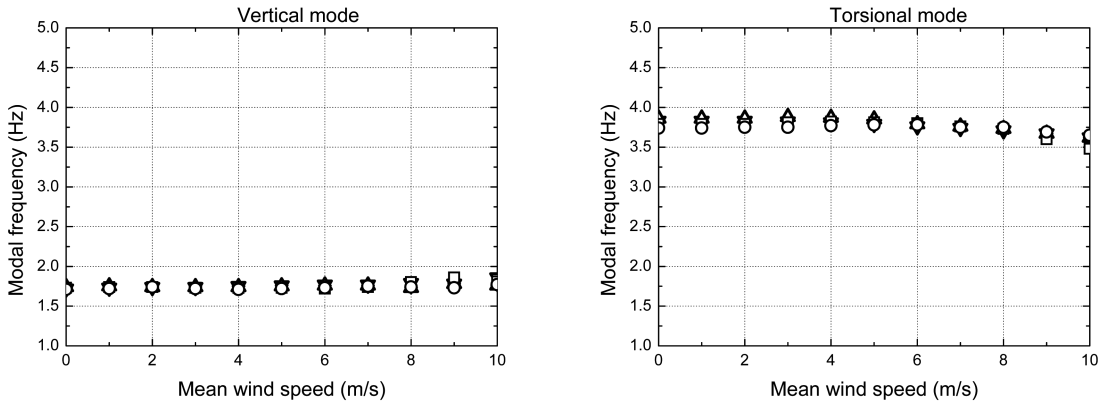

Fig. 6 Modal frequencies of models with different gap-widths
∇: Gap 1 +: Gap 2 Δ: Gap 3 □ : Gap 4 ○ : Gap 5

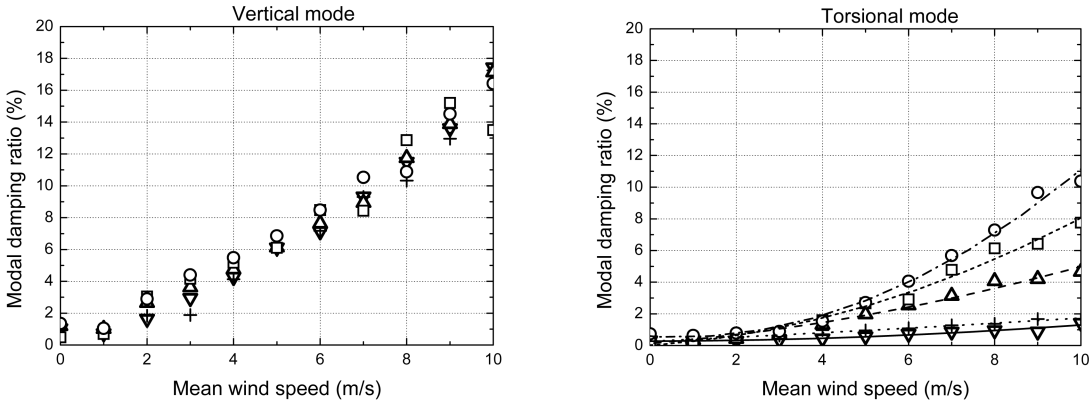

Fig. 7 Modal damping ratios of models with different gap-widths
∇: Gap 1 +: Gap 2 Δ: Gap 3 □ : Gap 4 ○ : Gap 5

vertical mode for each gap-width increased quickly with an increase of wind speed, although the differences between different gap-width configurations were comparatively small. The modal damping ratio of the torsional mode, however, was much more sensitive to gap-width and was enhanced significantly by increasing the gap-width above 16% of the bridge's total width, i.e. configurations denoted as Gap 3, Gap 4 and Gap 5, especially at the higher wind speeds. At 10 m/s, the maximum test wind speed, the modal damping ratio of the torsional mode for the configuration with the biggest gap-width (Gap 5) was about 10%, approximately 60% of the corresponding modal damping ratio of the vertical mode (around 16%). In comparison, for the zero gap-width configuration, at the maximum test wind speed, the modal damping ratio of the torsional mode was only approximately 1.5%, less than 10% of the corresponding damping ratio of the vertical mode (about 18%).

The mode shapes of the vertical and torsional complex modes can be defined as per Eq. (20) and Eq. (21), respectively, where the first subscript of each term corresponds to the degree-of-freedom and the second subscript corresponds to mode number. The mode shape matrix of the 2DOF bridge dynamic system therefore can be written as Eq. (22).

$$\{\phi\}_h = \begin{Bmatrix} A_{hh} \\ A_{\alpha h} \end{Bmatrix} \qquad \{\phi\}_\alpha = \begin{Bmatrix} A_{h\alpha} \\ A_{\alpha\alpha} \end{Bmatrix} \tag{20), (21}$$

$$[\Phi] = \begin{bmatrix} A_{hh} & A_{h\alpha} \\ A_{\alpha h} & A_{\alpha\alpha} \end{bmatrix} \tag{22}$$

Fig. 8 presents the amplitude ratios of the vertical and torsional complex modes of the 2DOF bridge dynamic system, for models with different gap-widths. The amplitude ratios of the vertical mode and torsional mode were defined as $c|A_{\alpha h}|/|A_{hh}|$ and $|A_{h\alpha}|/c|A_{hh}|$ respectively, where c is the chord width. Fig. 8 suggests that for all the five test models, the amplitude ratios of the vertical and torsional complex modes both were amplified with an increase of wind speed. However, comparing the trend for one gap-width to another, no remarkable difference of the amplitude ratios was

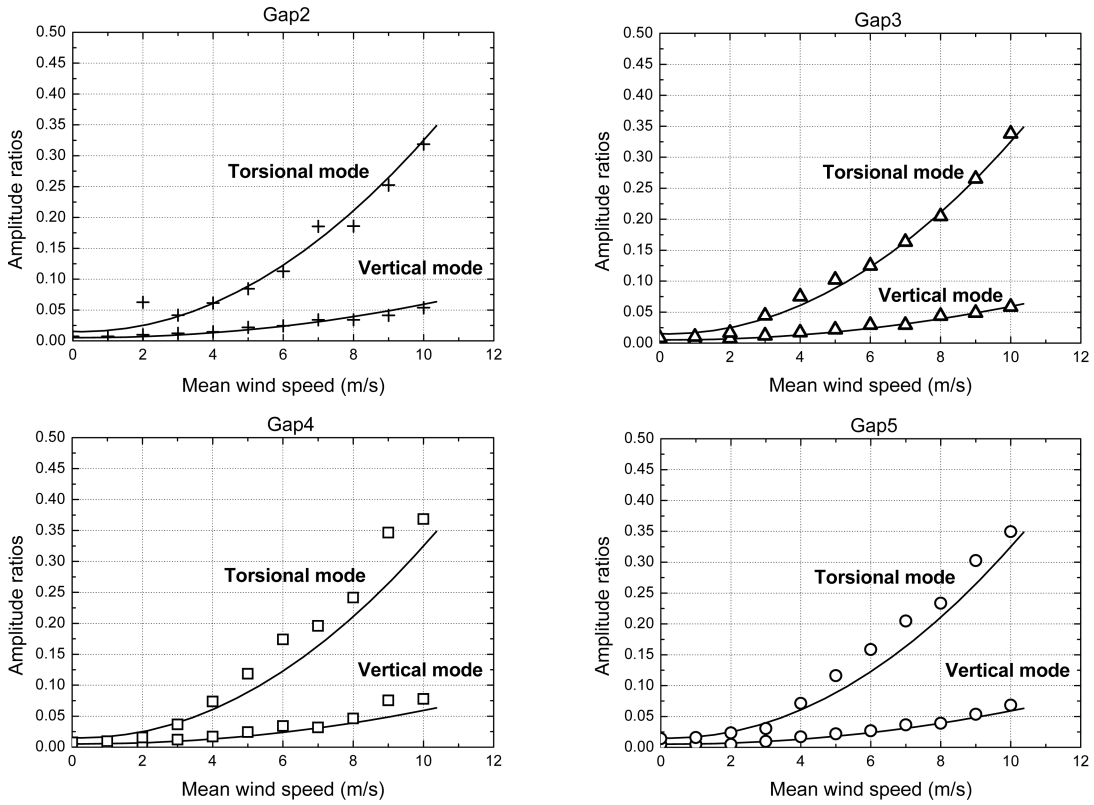

Fig. 8 Amplitude ratios of the vertical and torsional complex modes
——: Gap 1 (curve-fitted) +: Gap 2 Δ: Gap 3 □ : Gap 4 ○ : Gap 5

observed at all the test wind speeds.

Fig. 9 presents the phase differences of the vertical and torsional complex modes of the 2DOF bridge dynamic system, for models with different gap-widths. The phase differences between the vertical and torsional components for the vertical and torsional modes were defined as angle($A_{\alpha h}$) − angle(A_{hh}) and angle($A_{h\alpha}$) − angle($A_{\alpha\alpha}$), respectively. It is evident that gap-width shows much more effects on the phase differences, as compared to the amplitude ratios, of the vertical and torsional complex modes.

3.4. Identified dimensionless flutter derivatives

The eight dimensionless flutter derivatives related to the vertical bending and torsion motions of the 2DOF bridge dynamic model were simultaneously extracted from the coupled free-decay responses. Since H_4^* and A_4^*, the two flutter derivatives associated with the vertical displacement response, have proven to be very sensitive to the potential noise during wind tunnel tests (Gu, *et al.* 2001), and their influence on the flutter properties of bridges is very small (Iwamoto and Fujino, 1995), the relevant results were not reported in the current paper. Fig. 10 presents the six dimensionless flutter derivatives of the five bridge models with different gap-widths, where H_1^* and A_1^* were normalized by the actual vertical frequency of the bridge dynamic system at the specific

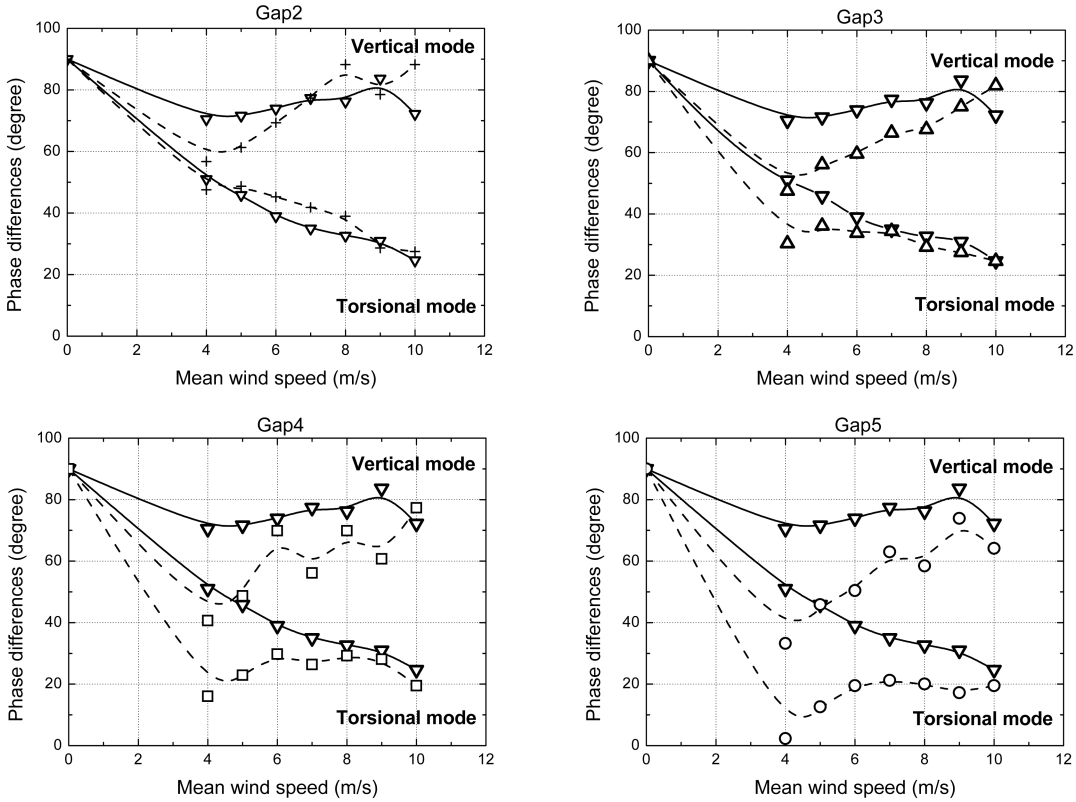

Fig. 9 Phase differences of the vertical and torsional complex modes
—— and ∇: Gap 1 ------ and +: Gap 2
------ and Δ: Gap 3 ------ and □ : Gap 4 ------ and ○ : Gap 5

test wind speed, while A_2^*, A_3^*, H_2^* and A_3^* were normalized by the actual torsional frequency, as shown in Eq. (17).

Each dimensionless flutter derivative of the five tested configurations was plotted with respect to the dimensionless reduced velocity *U*/*fB*, in which *f* is the actual vertical or torsional frequency (Hz) of the 2DOF bridge dynamic system at the specific test wind speed. Fig. 10 reflects that the effects of gap-width on H_1^* and H_3^* are negligible, and that the magnitude of A_2^* was magnified when the gap-width between the twin decks was increased from 0% (Gap 1) to 35% (Gap 5) of the total deck width, while the magnitudes of H_2^*, A_1^* and A_3^* were diminished. However, when the gap is increased from 16% (Gap 3) to 27% (Gap 4) and 35% (Gap 5) of the total deck width, the differences of the corresponding dimensionless flutter derivatives are quite small, and it is almost impossible to distinguish between A_2^* for Gap 3, Gap 4 and Gap 5.

3.5. Identified dimensional flutter derivatives

Since the dimensionless flutter derivatives were normalized by the total width of the bridge deck, i.e., B in Fig. 1, which is different for various models with different gap-widths, it is not convenient or reasonable to apply them to investigate the effects of gap-width on the self-excited force and

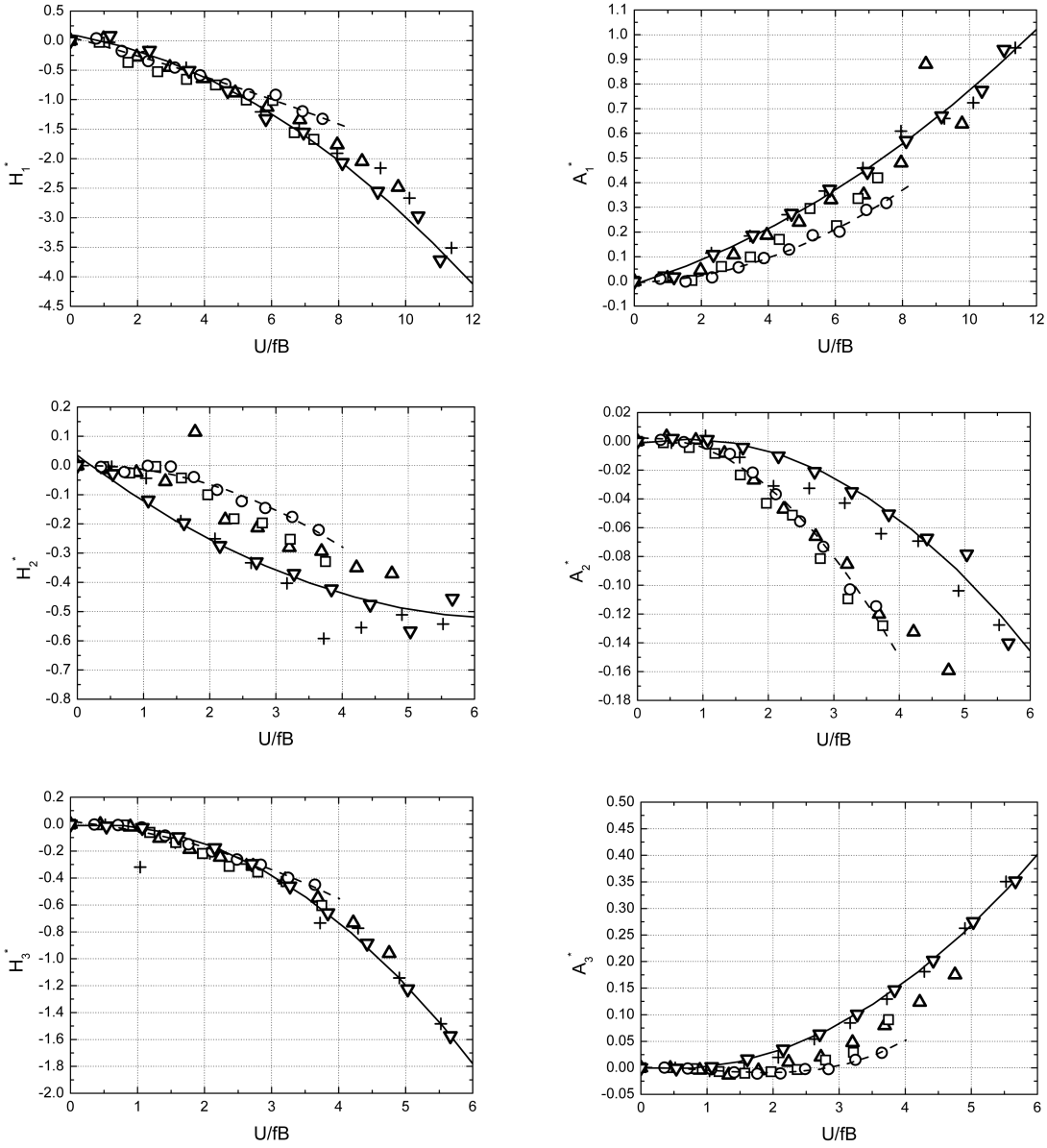

Fig. 10 Dimensionless flutter derivatives of models with different gap-widths

—— Gap 1 (curve fitted) ------ Gap 5 (curve fitted)

∇: Gap 1 +: Gap 2 Δ: Gap 3 □ : Gap 4 ○ : Gap 5

------ and Δ: Gap 3 ------ and □ : Gap 4 ------ and ○ : Gap 5

moment of bridges. In this case, alternative parameters should be utilized.

As stated in Scanlan's paper (1971), in some circumstances, it has been shown more convenient to replace the dimensionless flutter derivatives H_1^* and A_1^* by the dimensional coefficients listed in Eq. (23):

$$\begin{aligned} H_1 &= \frac{\rho B^2 \omega_h}{m} H_1^* \qquad A_1 = \frac{\rho B^3 \omega_h}{I} A_1^* \\ H_2 &= \frac{\rho B^3 \omega_\alpha}{m} H_2^* \qquad A_2 = \frac{\rho B^4 \omega_\alpha}{I} A_2^* \\ H_3 &= \frac{\rho B^3 \omega_\alpha}{m} H_3^* \qquad A_3 = \frac{\rho B^4 \omega_\alpha^2}{I} A_3^* \\ H_4 &= \frac{\rho B^2 \omega_h^2}{m} H_4^* \qquad A_4 = \frac{\rho B^3 \omega_h^2}{I} A_4^* \end{aligned} \tag{23}$$

The dimensional coefficients, H_i and A_i ($i=1,2,3,4$), correspond to the dimensional forms of flutter derivatives and are named "dimensional flutter derivatives" in the current study. The self-excited lift force and pitching moment therefore can be expressed as:

$$\begin{aligned} L_{se} &= m[H_1\dot{h}(t) + H_2\dot{\alpha}(t) + H_3\alpha(t) + H_4 h(t)] \\ M_{se} &= I[A_1\dot{h}(t) + A_2\dot{\alpha}(t) + A_3\alpha(t) + A_4 h(t)] \end{aligned} \tag{24}$$

Fig. 11 presents the six dimensional flutter derivatives H_1 to H_3 and A_1 to A_3 for models with different gap-widths. Instead of adopting the reduced velocity, as was the case for the dimensionless flutter derivatives, each of the dimensional flutter derivatives was plotted with respect to the test mean wind speed. In general, the trend of each resultant dimensional flutter derivative is quite consistent with that of the corresponding dimensionless flutter derivative, although the dimensional flutter derivatives show a relatively smaller degree of scatter.

Fig. 11 indicates that the flutter derivatives A_2 and A_3, corresponding to the torsional damping and stiffness respectively, are the most significantly affected by gap-width. As shown in Eq. (24), A_2 and A_3 are related to the contributions of various responses to the self-excited pitching moment. Evidently, the effects of gap-width are more prominent for the self-excited pitching moment than for the lift force.

When the gap-width between the twin decks was increased from 0% (Gap 1) to 35% (Gap 5) of the total deck width, the magnitude of A_2 was magnified, while the magnitude of A_3 was diminished. This trend corresponds to an enhanced contribution by the torsional velocity, while the contribution of torsional displacement was diminished.

It is evident from the definition of self-excited force, i.e., Eq. (2), that the free-vibrations of the 2DOF bridge dynamic system are aerodynamically coupled, including both damping coupling and stiffness coupling, and are represented by the off-diagonal terms, corresponding to flutter derivatives H_2, H_3 and A_1, in the effective damping and stiffness matrices. Fig. 11 suggests that the effect of gap-width on H_1 and A_1 are negligible, and that compared with A_2 and A_3, H_2 and H_3 are less sensitive to gap-width, which means that the effects of gap-width on the coupling between the vertical and torsional vibrations are less significant.

4. Concluding remarks

A series of wind tunnel dynamic model tests were conducted and system identification analyses

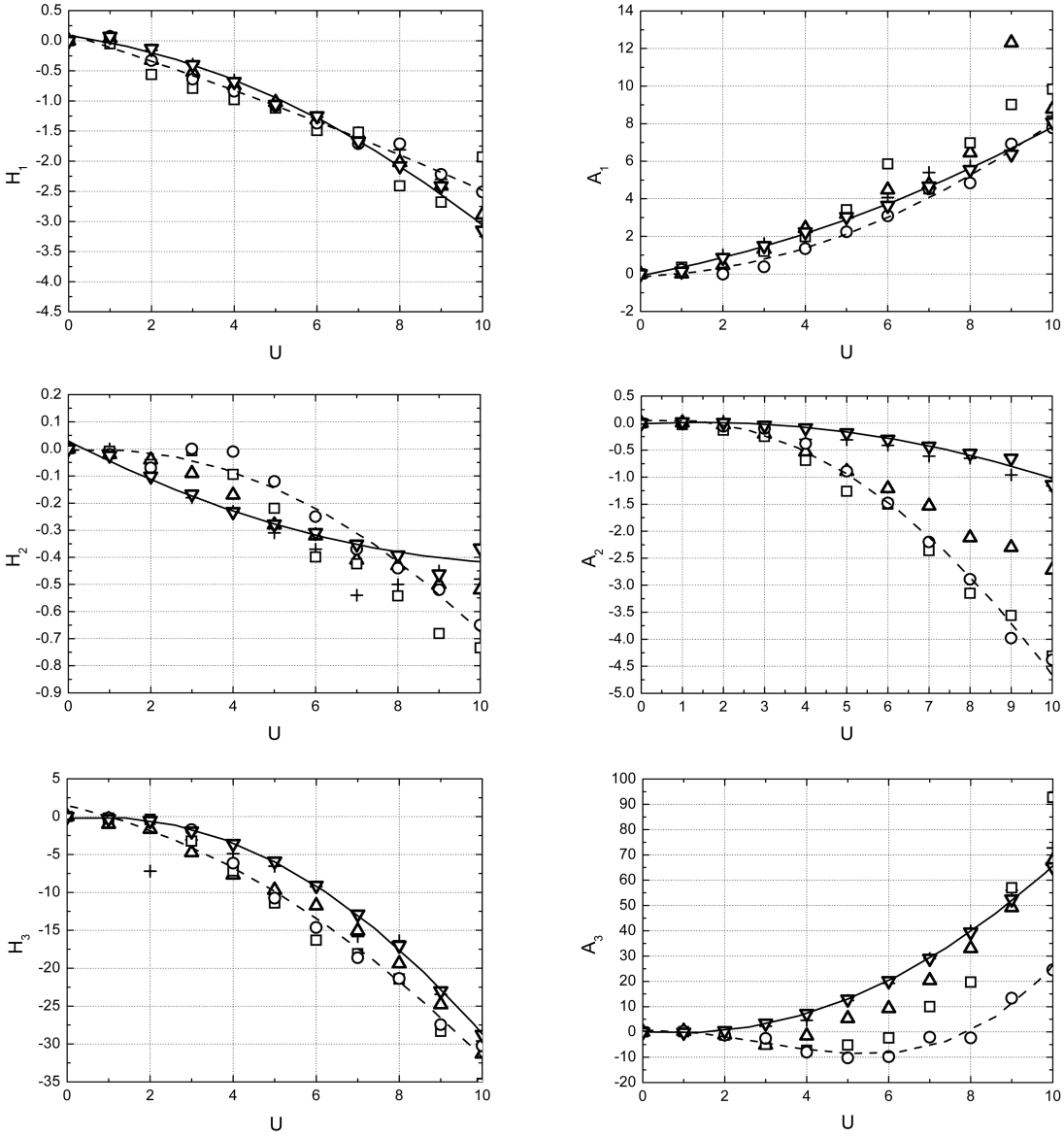

Fig. 11 Dimensional flutter derivatives of models with different gap-widths

—— Gap 1 (curve fitted) ------ Gap 5 (curve fitted)

∇: Gap 1 +: Gap 2 Δ: Gap 3 □ : Gap 4 ○ : Gap 5

were performed to investigate the effects of gap-width on the dynamic and aerodynamic characteristics of a real cable-stayed twin-deck bridge. Five 2.9 m long sectional models were fabricated and tested from 1 m/s up to the design mean wind speed of the bridge. The test results suggest that:

(i). A central gap contributes significantly to the torsional damping properties of the bridge. Increasing the gap-width has the potential to enhance the overall torsional damping and thus the aerodynamic stability of the bridge.

(ii). The relative size of a central gap affects the self-excited pitching moment more than the lift force.

(iii). For the tested 2DOF bridge dynamic system, with a large torsional-to-vertical frequency ratio (around 2.2), at wind speeds lower than the design mean wind speed of the prototype bridge, the relative size of a central gap affects the torsional damping and stiffness more than the coupling between the vertical and torsional vibrations.

Acknowledgements

This research was supported by the HKUST Targets of Opportunities Fund (Project: TOOF03/04.EG01) and Research Grants Council of Hong Kong (Project: PolyU1/02C-CA02/03.EG03), and Natural Science Foundation of China (Project: 50308022). The authors would also like to gratefully acknowledge the contributions of the Highways Department of the Hong Kong SAR.

References

Chen, X. and Kareem, A. (2004), "Efficacy of the implied approximation in the identification of flutter derivatives", *J. Struct. Eng.*, **130**(12), 2070-2074.

Gu, M., Zhang, R.X. and Xiang, H.F. (2000), "Identification of flutter derivatives of bridge decks", *J. Wind Eng. Ind. Aerodyn.*, **84**, 151-162.

Gu, M., Zhang, R.X. and Xiang, H.F. (2001), "Parametric study on flutter derivatives of bridge decks", *Eng. Struct.*, **23**, 1607-1613.

Iwamoto, M. and Fujino, Y. (1995), "Identification of flutter derivatives of bridge deck from free vibration data", *J. Wind Eng. Ind. Aerodyn.*, **54/55**, 55-63.

Juang, J.N. and Pappa, R.S. (1985), "An eigensystem realization algorithm for modal parameter identification and model reduction", *J. Guidance, Control and Dynamics*, **8**(5), 620-627.

Matsumoto, M., Shijo, R., Eguchi, A., Hikida, T., Tamaki, H. and Mizuno, K. (2004), "On the flutter characteristics of the separated two box girders", *Wind Struct.*, **7**(4), 281-291.

Qin, X.R. and Gu, M. (2004), "Determination of flutter derivatives by stochastic subspace identification technique", *Wind Struct.*, **7**(3), 173-186.

Sarkar, P.P., Jones, N.P. and Scanlan, R.H. (1994), "Identification of aeroelastic parameter of flexible bridges", *J. Eng. Mech., ASCE*, **120**(8), 1718-1741.

Sato, H., Toriumi, R. and Kasakabe, T. (1995), "Aerodynamic characteristics of slotted box girders", *Proceedings of Bridge into the 21st Century*, Hong Kong, pp. 721-728.

Sato, H., Kusuhara, H., Ogi, K. and Matsufuji, H. (2000). "Aerodynamic characteristics of super long-span bridges with slotted box girder", *J. Wind Eng. Ind. Aerodyn.*, **8**(8), 297-306.

Scanlan, R.H. (1971), "Airfoil and bridge deck flutter derivatives", *J. Eng. Mech., ASCE*, EM6, pp. 1717-1737.

Xiang, H.F. and Ge, Y.J (2002), "Refinements on aerodynamic stability analysis of super long-span bridges", *J. Wind Eng. Ind. Aerodyn.*, **90**, 1493-1515.

JH